Experimental Investigation of Friction Stir Welding of Dissimilar Aluminium Alloys using RSM Technique

Manmohan[1] Sandeep Kumar[2]
[1,2]Samalkha Group of Institutions, Samalkha, India

Abstract— Friction Stir Welding is a solid state thermo mechanical joining process that involves joining of metals without fusion or filler materials. The process is particularly applicable for aluminium alloys by using conventional milling machine but can be extended to other products also. Plates, sheets and hollow pipes can be welded by this method. The frictional heat is produced from a rapidly rotating non-consumable high strength tool pin that extends from a cylindrical shoulder. The process is also suitable for automation. The overall aim of this study is to get the optimum parameters for the materials under considerations Tool rotational speed (A), Welding speed (B) and Tool tilt angle(C) to investigate the Ultimate tensile strength(R1), Yield Tensile strength(R2) & Percentage Elongation(R3).

NOMENCLATURE

- FSW: Friction stir welding,
- A: Tool rotational speed, rpm
- B: welding speed, mm/sec
- C: Welding tool tilt angle, Degree
- T: Plate thickness, mm
- R1: Ultimate Tensile Strength
- R2:Yield Tensile strength, MPa
- R3: Percentage Elongation, %
- RSM: response surface methodology
- TWI: The Welding Institute

Key words: Friction Stir Welding, Aluminium Alloys, RSM Technique

I. INTRODUCTION

Friction Stir Welding (FSW) is another joining procedure in which no exhaust, utilizes no filler material, Eco-friendly and can join a few metal combinations, for example, aluminum, magnesium, copper, steels, titanium and zinc. In 1991 a possibly world beating welding strategy was found at The Welding Institute (TWI). The procedure was named Friction Stir Welding (FSW), and The Welding Institute (TWI) petitioned for overall patent assurance in December of that year. TWI is a world acclaimed initiate in the UK that has practical experience in materials welding innovation. Steady with the more regular strategies for Friction Stir Welding, which have been practiced since the mid-1950s, the weld is made in the strong stage, that is, no dissolving is included as Compared to traditional welding.

FSW some of the time delivers a weld that is more grounded than the base material. FSW is a solid state joining process, where metal isn't softened utilizations a cylindrical shaped, tool with a profiled test pivoted and gradually inserted into the weld joint between two metal bits of sheet or plate that are to be welded together . The parts must be fixed onto a specially design fixture in a way that keeps the adjoining joint appearances from being constrained separated or in some other path moved out of position. Frictional heat is created between the tool and material causing the work pieces to mellow without achieving the melting point, and afterward mechanically intermixes the two pieces of metal at the place of the joint, additionally diminished metal because of the lifted temperature is joined utilizing mechanical weight, connected by the tool. This leaves a strong stage bond between the two pieces. Since softening does not happen and joining happens beneath the dissolving temperature of the material, a brilliant weld is made. This trademark incredibly diminishes the evil impacts of high temperature input, including friction, and dispensing with cementing absconds. The procedure initially was constrained to low softening temperature materials since introductory tool materials couldn't hold up to the worry of friction higher temperature materials, for example, steels and its combinations, other high-quality materials. This issue was tended to as of late with the presentation of new tool material advancements, for example, polycrystalline cubic boron nitride (PCBN), tungsten rhenium, and pottery. The utilization of a fluid cooled tool holder and telemetry framework has additionally refined the procedure and capacity. Tool materials required for FSW of high-liquefying temperature materials require high "hot" hardness for scraped area protection, alongside synthetic soundness and satisfactory strength at high temperature. Material advancements are progressing quickly in various tool materials, every material offering particular points of interest for various applications.

FSW utilizes a pivoting tool to produce the vital heat for the procedure. Since its creation, the procedure has gotten overall consideration and today two Scandinavian organizations are utilizing the innovation underway, especially to join aluminum alloys. Additionally, FSW is a procedure that can be mechanized. It is additionally a cleaner and more productive process contrasted with ordinary procedures.

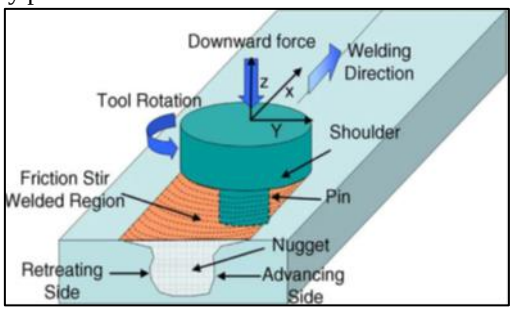

Fig. 1: Schematic Drawing of Friction Stir Welding

Friction Stir Welding (FSW) is a genuinely latest procedure that uses a non-consumable turning welding tool to produce frictional warmth and plastic deformation at the welding area, in this manner influencing the development of a joint while the material is in the strong state. The pivoting tool is pushed against the surface of two butted plates. The side of the weld for which the tool moves an indistinguishable way from the navigating bearing, is usually known as the propelling side, theopposite side,

where device pivot contradicts the crossing heading is referred to as the withdrawing side as appeared in the Fig. 1.

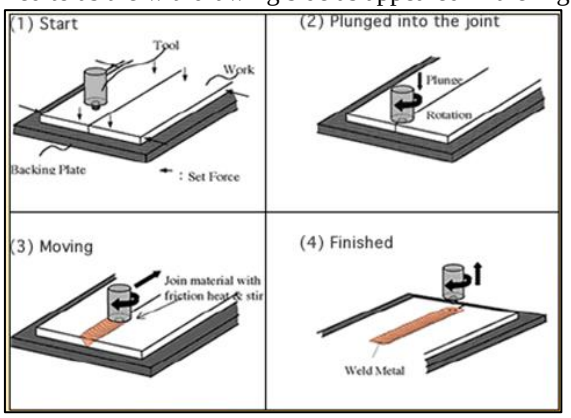

Fig 2: Friction Stir Welding Steps

It is a strategy for strong stage welding, which permits an extensive variety of parts and geometries to be welded are called Friction Stir Welding (FSW), as of late, concentrate has been on growing quick, proficient procedures that are eco-friendly to join two materials.

The spotlight has been turned on Friction stir welding as a joining innovation fit for giving welds that don't have surrenders regularly connected with combination welding forms. The procedure demonstrates greater part to weld non-heating treatable to which the dissemination (circular segment welding) welding can't be obtained. Friction stir welding has a wide application in dispatch building, aviation, car and other assembling enterprises. In this manner crucial thinks about on the weld system, the welding between microstructure, mechanical properties and process parameters have as of late been begun.

II. MATERIAL COMPOSITION

A. Aluminum 7039 Alloy

Aluminium is one of the lightest available commercial metals with a density approximately one-third that of steel or copper. It can be easily fabricated into many forms such as foil, sheets, rod, tube, geometric shapes, and wire.

Here AA7039, AA5083 is used as work material and tool material is H13. Following are the details of chemical Composition of all materials.

Element	Content (%)
Zinc, Zn	3.5-4.5
Magnesium, Mg	2.3-3.3
Silicon, Si	0.3 max
Iron, Fe	0.4 max
Chromium, Cr	0.15-0.25
Manganese, Mn	0.1-0.4
Copper, Cu	0.1 max
Titanium, Ti	0.1 max
Remainder (total)	0.15 max
Aluminum, Al	Remainder

Table 1: Chemical Composition of AA7039

Element	Content (%)
Si	0.4
Fe	0.4
Cu	0.1
Mn	0.41.0
Mg	4.04.9
Zn	0.25
Ti	0.15
Cr	0.050.25
Al	Remainder

Table 2: Chemical Composition of AA5083

Element	Content
Carbon	0.32 - 0.45
Chromium	4.75 - 5.5
Manganese	0.2 - 0.5
Molybdenum	1.1 - 1.75
Phosphorus	0.03 max
Silicon	0.8 - 1.2
Sulphur	0.03 max
Vanadium	0.8 - 1.2

III. MACHINE SET UP FOR FSW

In friction stir welding (FSW) a cylindrical, shouldered tool with a square profiled probe is rotated and slowly plunged into the joint line between two pieces butted together. The parts have to be clamped onto a backing bar in a manner that prevents the abutting joint faces from being forced apart. Frictional heat is generated between the wear resistant welding tool and the material of the work pieces. This heat causes the latter to soften without reaching the melting point and allows traversing of the tool along the weld line as shown in the Figure-3The maximum temperature reached is of the order of 0.8 of the melting temperature of the material. The plasticized material is transferred from the leading edge of the tool to the trailing edge of the tool probe and is forged by the intimate contact of the tool shoulder and the pin profile. It leaves a solid phase bond between the two pieces. The process can be regarded as a solid phase keyhole welding technique since a hole to accommodate the probe is generated, then filled during the welding sequence.

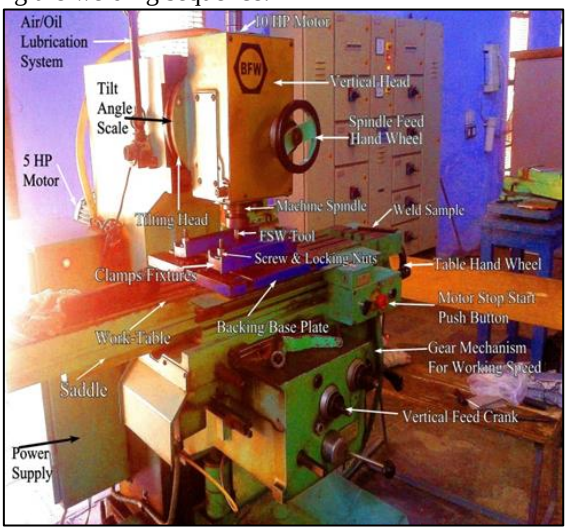

Fig. 3: Machine set up for FSW

A. Principle of Operation

Actual working diagram in Fig. 4. At first, the sheets or plates are abutted along edge to be welded and the rotating

pin is sunken into the sheets/plates until the tool shoulder is in full contact with the sheets or plates surface. Once the pin is completely inserted, it is moved with a small notating angle in the welding direction.

Due to the advancing and rotating effect of the pin and shoulder of the tool along the seam, an advancing side and a retreating side are formed and the softened and heated material flows around the pin to its backside where the material is consolidated to create a high-quality.

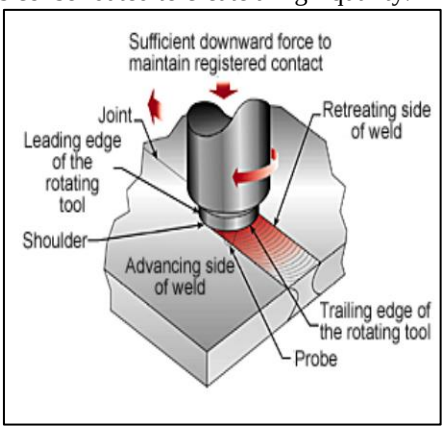

Fig. 4: Principle Operation of FSW

B. Experimental Work

This chapter discusses the results obtained and optimizes the FSW process parameter using RSM method. The objective function is to maximize the tensile strength and percentage elongation of the FSW joint. The optimum levels of the proc ess parameters are calculated and confirmed by conducting confirmation run. The effect of FSW process parameters such as rotational Speed, transverse speed, and Tool Tilt angle on tensile strength and percentage elongation are discussed.

The experimental results for Ultimate Tensile Strength (R1), Yield Tensile Strength (R2) and Percentage elongation (R3) are exemplified in Table 7. The analysis of variance (ANOVA) test was also executed with a view to examine the significance of the developed models. The ANOVA test results for considered process responses are detailed in Tables 8, 9 and 10.

Std.	Run	Block	Rotating Speed(rpm)	Welding Speed (mm/min)	Tilt Angle (degree)
3	1	Block 1	1000	50	3
7	2	Block 1	1500	35	2
2	3	Block 1	2000	20	3
1	4	Block 1	2000	50	1
6	5	Block 1	1500	35	2
5	6	Block 1	1500	35	2
4	7	Block 1	1000	20	1
11	8	Block 2	1500	50	2
10	9	Block 2	1500	20	2
13	10	Block 2	1500	35	3
14	11	Block 2	1500	35	2
16	12	Block 2	1500	35	2
12	13	Block 2	1500	35	1
8	14	Block 2	1000	35	2
15	15	Block 2	1500	35	2
9	16	Block 2	2000	35	2

Table 4: Process Parameter

Std	Run	Block	Factor 1 A:A	Factor 2 B:B	Factor 3 C:C	Response 1 R1	Response 2 R2	Response 3 R3
3	1	Block 1	-1.00	1.00	1.00	304.1	254.2	12.9
7	2	Block 1	0.00	0.00	0.00	403.8	339.2	18.2
1	3	Block 1	1.00	1.00	-1.00	234.4	198.6	10.2
2	4	Block 1	1.00	-1.00	1.00	235.6	199.2	10.4
6	5	Block 1	0.00	0.00	0.00	399.8	339.8	18.2
4	6	Block 1	-1.00	-1.00	-1.00	229.7	199.2	9.94
5	7	Block 1	0.00	0.00	0.00	402.8	348.1	18.9
9	8	Block 2	1.00	0.00	0.00	333.4	296	13.3
16	9	Block 2	0.00	0.00	0.00	403.8	337.4	16.3
15	10	Block 2	0.00	0.00	0.00	394.4	337.1	15.6
14	11	Block 2	0.00	0.00	0.00	400.4	336.1	16.1
13	12	Block 2	0.00	0.00	1.00	383.4	312.3	16.33
11	13	Block 2	0.00	1.00	0.00	350.7	291.2	14.91
10	14	Block 2	0.00	-1.00	0.00	317.3	275.6	13.49
8	15	Block 2	-1.00	0.00	0.00	365.5	309.6	15.82
12	16	Block 2	0.00	0.00	-1.00	350.7	299.3	14.91

Table 5: Results of FSW using RSM Technique

C. Result & Discussion

The Model F-value of 502.81 implies the model is significant. There is only a 0.01% chance that a "Model F-Value" this large could occur due to noise.

	Sum of		Mean	F	p-value	
Source	Squares	df	Square	Value	Prob > F	
Block	10193.04	1	10193.04			
Model	50542.15	9	5615.79	502.81	< 0.0001	Significant
A-A	515.21	1	515.21	46.12	0.0011	
B-B	557.78	1	557.78	49.94	0.0009	
C-C	534.64	1	534.64	47.87	0.001	
AB	8.67	1	8.67	0.78	0.4186	
AC	3.41	1	3.41	0.31	0.6042	
BC	0.013	1	0.013	1.19 E-03	0.9738	

A^2	6655.32	1	6655.32	595.89	< 0.0001	
B^2	11299.15	1	11299.15	1011.68	< 0.0001	
C^2	2854.04	1	2854.04	255.54	< 0.0001	
Residual	55.84	5	11.17			
Lack of Fit	1.87	1	1.87	0.14	0.7286	not significant
Pure Error	53.97	4	13.49			
Cor Total	60791.04	15				
Std. Dev.	3.34		R-Squared	0.9988		
Mean	344.36		Adjusted R^2	0.9969		
C.V. %	0.97		Pred R^2	0.9818		
PRESS	917.41		Adeq Precision	62.099		

Table 6: ANOVA for response R1 (UTS)

Values of "Prob > F" less than 0.0500 indicate model terms are significant. In this case A, B, C, A2, B2, C2 are significant model terms.

Values greater than 0.1000 indicate the model terms are not significant.

If there are many insignificant model terms (not counting those required to support hierarchy),

Model reduction may improve your model.

The "Lack of Fit F-value" of 0.14 implies the Lack of Fit is not significant relative to the pure

Error. There is a 72.86% chance that a "Lack of Fit F-value" this large could occur due

to noise. Non-significant lack of fit is good -- we want the model to fit.

The "Pred R-Squared" of 0.9819 is in reasonable agreement with the "Adj R-Squared" of 0.9969.

"Adeq Precision" measures the signal to noise ratio. A ratio greater than 4 is desirable. The

Ratio of 62.100 indicates an adequate signal. This model can be used to navigate the design space.

	Sum of		Mean	F	p-value	
Source	Squares	df	Square	Value	Prob > F	
Block	7006.26	1	7006.26			
Model	34871.23	6	5811.87	179.41	< 0.0001	significant
A-A	798.11	1	798.11	24.64	0.0011	
B-B	816.67	1	816.67	25.21	0.001	
C-C	784.33	1	784.33	24.21	0.0012	
A^2	3561.45	1	3561.45	1.10E+02	< 0.0001	
B^2	8229.11	1	8229.11	254.03	< 0.0001	
C^2	3011.64	1	3011.64	92.97	< 0.0001	
Residual	259.15	8	32.39			
Lack of Fit	208.74	4	52.18	4.14	0.0988	not significant
Pure Error	50.41	4	12.6			
Cor Total	42136.64	15				
Std. Dev.	5.69		R-Squared	0.9926		
Mean	292.06		Adj R^2	0.9871		
C.V. %	1.95		Pred R^2	0.945		
PRESS	1932.27		Adeq Precision	34.805		

Table 7: ANOVA for response R2 (YTS)

The Model F-value of 1 79.41 implies the model is significant. There is only a 0.01% chance that a "Model F-Value" this large could occur due to noise.

Values of "Prob > F" less than 0.0500 indicate model terms are significant. In this case A, B, C, A2, B2, C2 are significant model terms.

Values greater than 0.1000 indicate the model terms are not significant. If there are many insignificant model terms (not counting those required to support hierarchy), model reduction may improve your model.

The "Lack of Fit F-value" of 4.14 implies there is a 9.88% chance that a "Lack of Fit F-value" this large could occur due to noise. Lack of fit is bad -- we want the model to fit.

This relatively low probabiity (<10%) is troubling.

The "Pred R-Squared" of 0.9450 is in reasonable agreement with the "Adj R-Squared" of 0.9871.

"Adeq Precision" measures the signal to noise ratio. A ratio greater than 4 is desirable.Theratio of 34.805 indicates an adequate signal. This model can be used to navigate the design space.

Source	Squares	df	Square	Value	Prob > F	
Block	4.68	1	4.68			
Model	110.53	6	18.42	34.08	< 0.0001	significant
A-A	3.78	1	3.78	6.99	0.0296	
B-B	2.91	1	2.91	5.39	0.0488	

C-C	3.5	1	3.5	6.47	0.0345	
A^2	17.39	1	17.39	3.22E+01	0.0005	
B^2	22.52	1	22.52	41.68	0.0002	
C^2	6.12	1	6.12	11.33	0.0098	
Residual	4.32	8	0.54			
Lack of Fit	3.74	4	0.93	6.37	0.0502	not significant
Pure Error	0.59	4	0.15			
Cor Total	119.53	15				
Std. Dev.	0.74		R-Squared	0.9624		
Mean	14.72		Adj R^2	0.9341		
C.V. %	4.99		Pred R^2	0.8387		
PRESS	18.52		Adeq Precision	15.351		

Table 8: ANOVA for Response R3 (% Eongation)

The Model F-value of 34.08 implies the model is significant. There is only a 0.01% chance that a "Model F-Value" this large could occur due to noise.

Values of "Prob > F" less than 0.0500 indicate model terms are significant. In this case A, B, C, A2, B2, C2 are significant model terms.

Values greater than 0.1000 indicate the model terms are not significant. If there are many insignificant model terms (not counting those required to support hierarchy), model reduction may improve your model.

The "Lack of Fit F-value" of 6.37 implies there is a 5.02% chance that a "Lack of Fit F-
Value" this large could occur due to noise. Lack of fit is bad -- we want the model to fit.
This relatively low probabiity (<10%) is troubling.

The "Pred R-Squared" of 0.8387 is in reasonable agreement with the "Adj R-Squared" of 0.9341.

"Adeq Precision" measures the signal to noise ratio. A ratio greater than 4 is desirable. Your Ratio of 15.351 indicates an adequate signal. This model can be used to navigate the design space.

D. Checking the Adequacy of Anova Model for Response, R1, R2 and R3

On the basis of the ANOVA test outcomes detailed in Tables 6, 7 and 8, the values of the probability term ‘‘Prob>F’’ (<0.0500) has statistically confirmed the significance of model terms at 95% confidence interval level. The models with F-values of 502.81, 179.41 and 34.08 entail that three models are statistically substantial and fits the data more satisfactorily. For the models, ‘‘p-value’’ is 0.7286 (Response R1 i.e. UTS) and 0.0988 (Response R2 i.e. YTS) and 0.0502 (Response R3 i.e. Elongation %) for the term ‘‘lack of fit,’’ which confirms it as an irrelevant term in perspective to the pure error. The percent involvement for all the models has also been computed as the ratio of the term ‘‘sum of squares’’ for individual source to the ‘‘total of sum of squares.’’. This quite smaller magnitude of pure error for all the three models reveals that there is nearly negligible deviation in the experimental results caused by error. ‘‘R-Square’’ (called as ‘‘coefficient of determination’’) is another imperative coefficient in the ANOVA analysis. Developed model entails best elucidation of experimental data, if the value of ‘’R-Square’’ term approaches unity. The computed values of 0.9988, 0.9926 and 0.9624 in Tables 6, 7 and 8, correspondingly, signifies that model explicates 99.88%, 99.26% and 96.24 variability of R1, R2 and R3, respectively.

To make confirm, whether the model has described the well relationship between process variables and considered responses (i.e. R1, R2 and R3) or not, the ‘‘predicted R-Square’’ and ‘‘adjusted R-Square’’ has been examined. For R1, R2 and R3, the values of the predicted “R-Square” (0.9818, 0.9450, and 0.8387) demonstrate rational concurrence with “adjusted R-Square’’ (0.9847 and 0.8740), correspondingly. The ratio of signal-to-noise (S/N ratio) is exemplified through the term ‘‘adequate precision.’’ The model will be fit to proceed further, if the value of ‘‘adequate precision’’ is greater than 4. The ratios of 62.099, 34.805 and 15.351 designate satisfactory indications for developed Ultimate Tensile Strength (R1), Yield Tensile Strength (R2) and Percentage Elongation (R3) models, respectively. The fraction of the standard deviation to mean is called as— ‘‘coefficient of variation (CV),’’ which elucidates the relative variation for R1, R2 and R3 the values of ‘‘coefficient of variation’’ are 0.97%, 1.95 and 4.99%, respectively, which further specifies admirable accuracy and reliability of the experimentation conducted. Based on RSM approach, the developed models for R1, R2 and R3 are represented after employing method of ‘‘backward elimination’’ for obliterating ‘‘not significant’’ variables

Figure 5, 8 and 11 illustrates the normal probability Plots of the residuals for Response R1(UTS), R2(YTS) and R3 (% Elongation) These plots reveal that most of the residuals are scattered out along the best fitted line, which further confirms the normally dispersing of the errors. Validation of the developed models is made by analyzing actual values with predicted values. Figures 6, 9 and 12 shows the actual values versus predicted values plots for all the three investigated responses, i.e. R1, R2 and R3, respectively. As interpreted from these plots, the developed regression models are satisfactorily attuned with the actual values. Therefore, the prediction made with the developed second-order regression models for considered responses (i.e. R1, R2 and R3) is validated with accuracy and constancy.

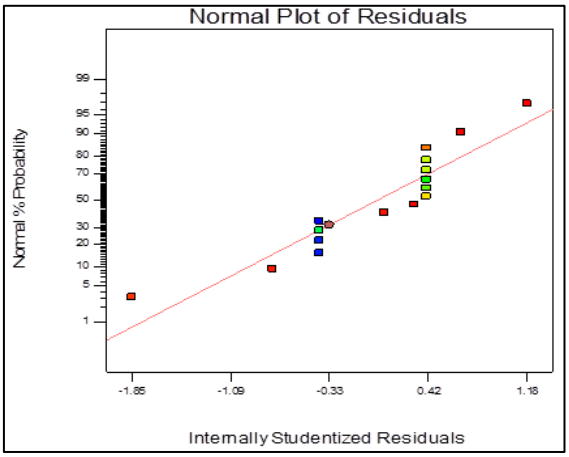

Fig. 5: Normal Plot of Residual for R1

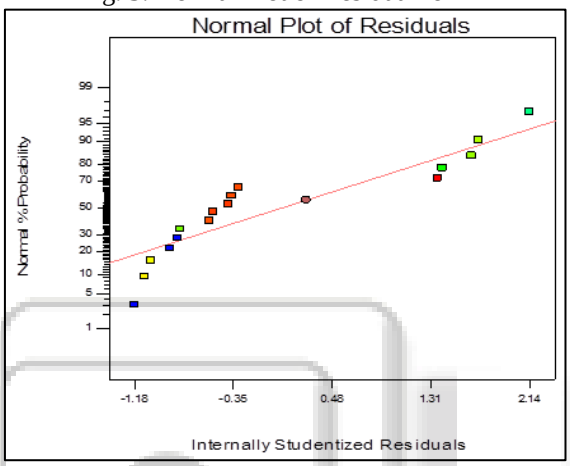

Fig. 6: Normal Plot of Residual for R2

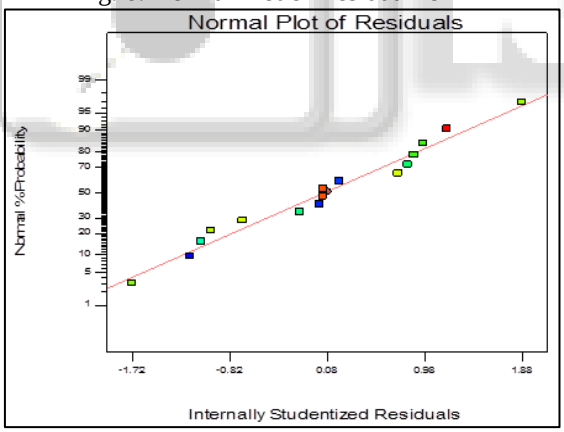

Fig. 7: Normal Plot of Residual for R3

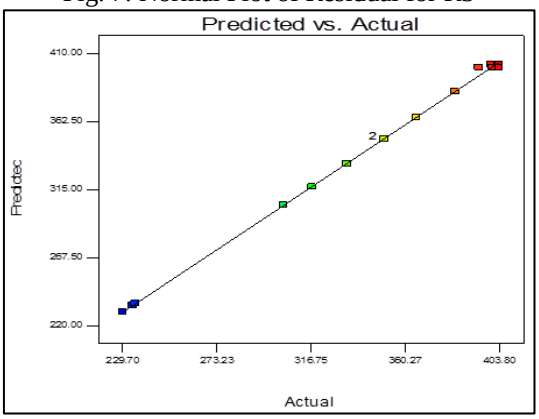

Fig. 8: Graph Plotted Predicted Vs. Actual for R1

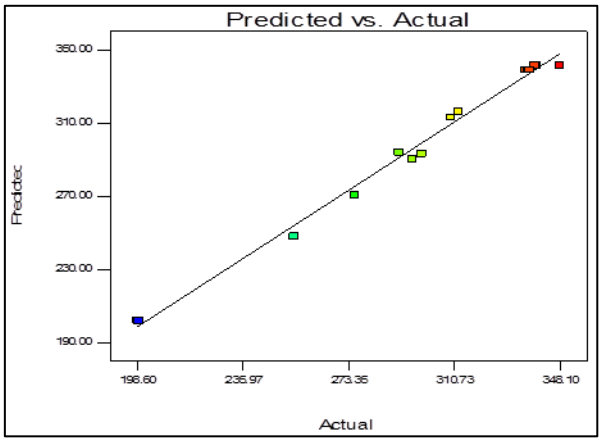

Fig. 9: Graph Plotted Predicted Vs. Actual for R2

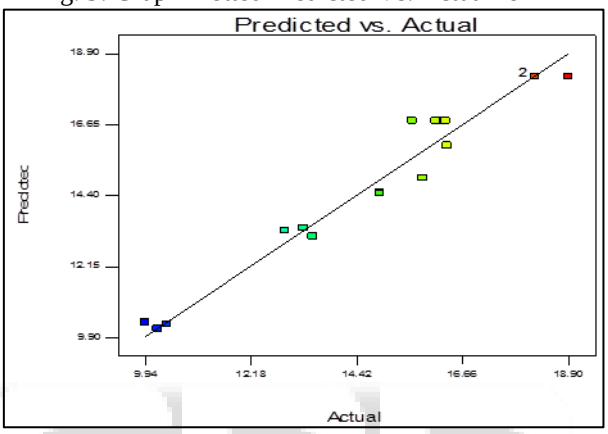

Fig. 10: Graph Plotted Predicted Vs. Actual for R3

In fig.10 to 12 the perturbation shows that the when the rotational speed of tool is increased the value of, R1 (UTS), R2 (YTS) and R3 (% Elongation) increases and then it tends to decrease. Also when the welding speed is increased then the value of, R1 (UTS), R2 (YTS) and R3 (% Elongation) also increases up to a certain point then it also turned to decrease. Same case repeated for the tilt angle, when tilt angle increased the value of, R1 (UTS), R2 (YTS) and R3 (% Elongation) also increases but after a certain limit to also tends to decrease. Hence From perturbation diag. a suitable value is selected which gives the most significant value.

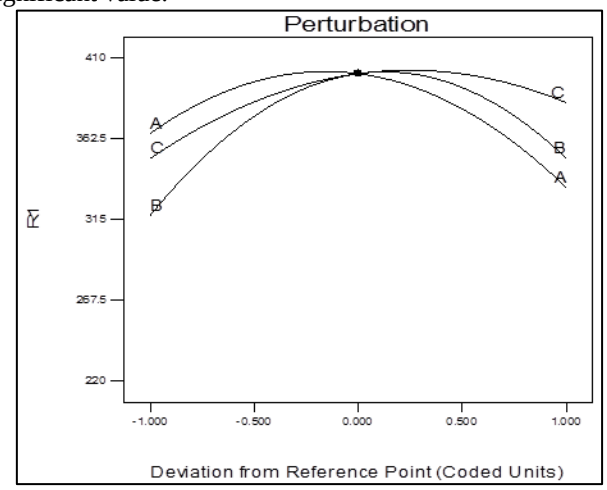

Fig. 11: Graph Plotted of Perturbation for R1

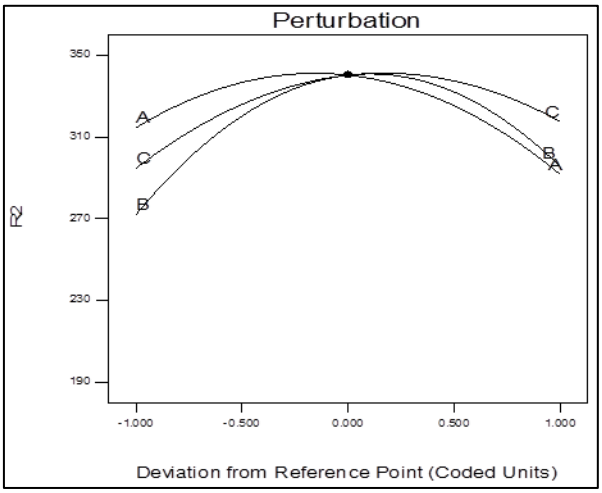

Fig. 12: Graph Plotted of Perturbation for R2

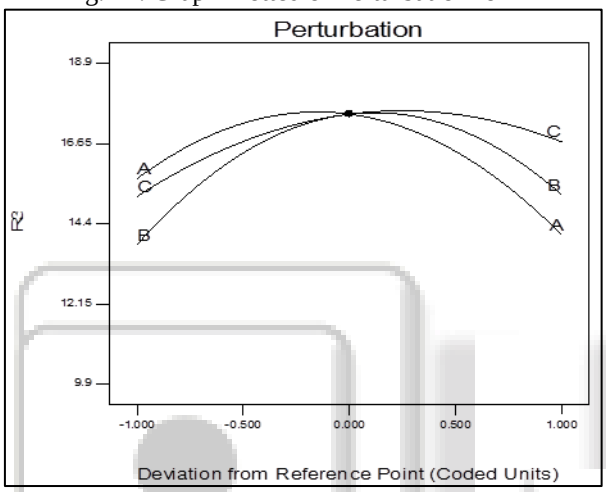

Fig. 13: Graph Plotted of Perturbation for R3

E. Analysis of the Response Surface Plots and Contour Plots

Ultimate tensile strength of FS welded aluminium alloy AA 5083 and AA 7039 were predicted by the mathematical models using the experimental observations presented in Figs. 5 to 11, circumstances and end results. From Figs. 13 and 16, it is seen that as the rotational speed increases the tensile strength of FS welded AA 5083 and AA 7039 increases and then decreases. It is clear that in FSW as the rotational speed increases, the heat generated increases. In the meantime, low rotational speed delivers low heat, which brings about the absence of stirring activity, thus the quality is low. From Figs.13 and 18, it is evident that as welding speed increases from 20 mm/min to 50 mm/min, the tensile strength of the FS welded aluminum alloy AA 5083 and AA 7039 increases and then decreases. At the lowest welding speed (20 mm/min) and highest welding speed (50 mm/min), lower tensile strength is observed. This is due to the increased frictional heat and insufficient frictional heat generated respectively.

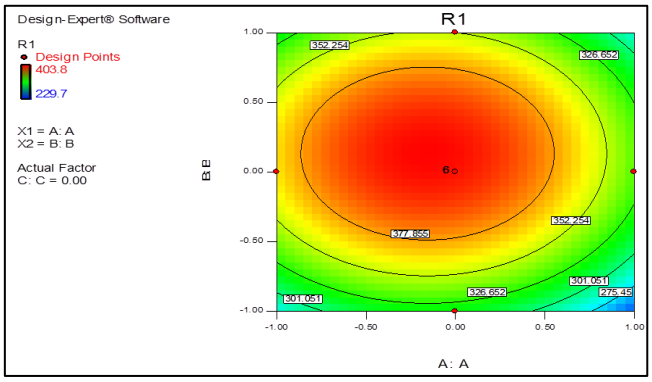

Fig. 14: Contour Plots of Tool Rotational Speed and welding speed on R1 (UTS)

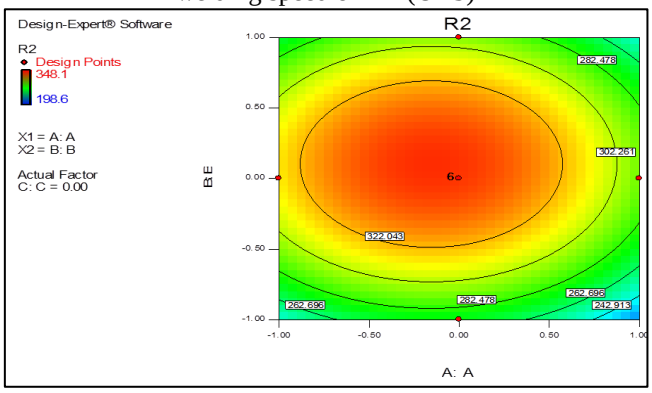

Fig. 15: Contour Plots of Tool Rotational Speed and Welding Speed on R2 (YTS)

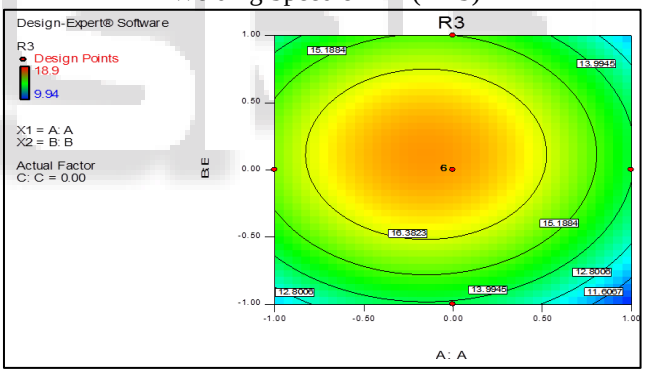

Fig. 16: Contour Plots of Tool Rotational Speed and Welding Speed on R3 (% Elongation)

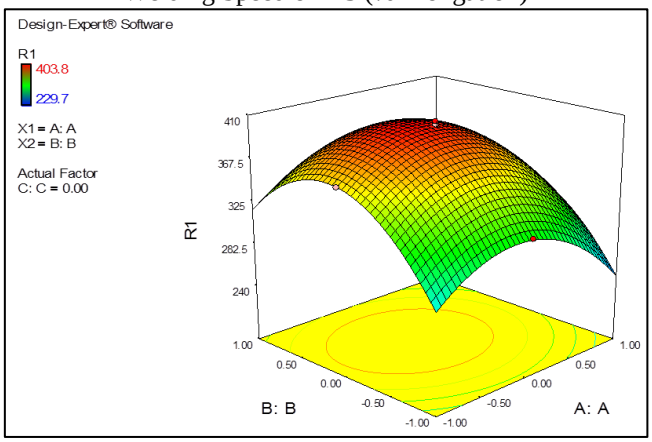

Fig. 17: Response Surface Graphs of Rotational Speed and Welding Speed on R1 (UTS)

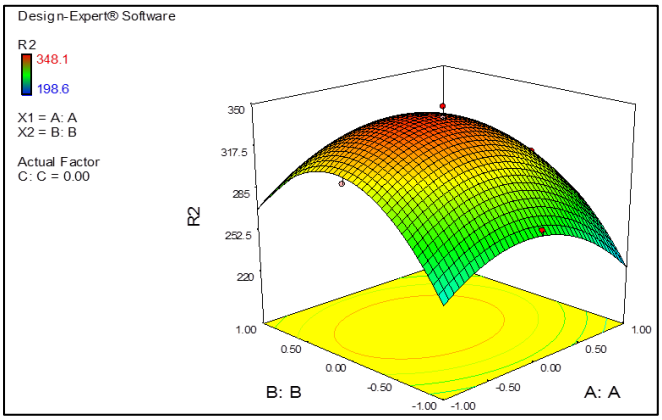

Fig. 18: Response Surface Graphs of Rotational Speed and Welding Speed on R2 (YTS)

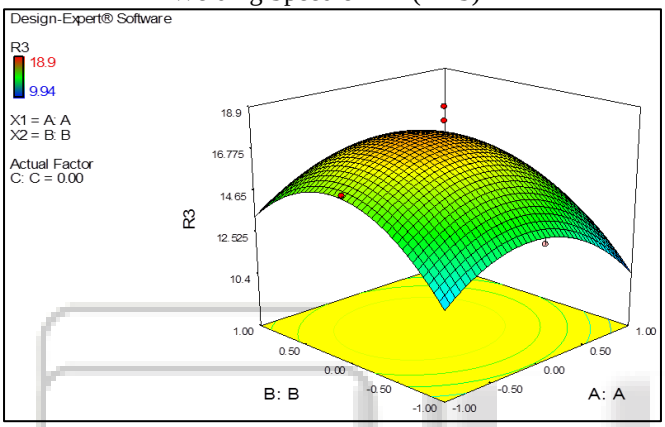

Fig. 19: Response Surface Graphs of Rotational Speed and Welding Speed on R3 (% Elongation)

IV. CONCLUSION

- FSW of 7039 and 5083 was conducted successfully
- ANOVA results for UTS(R1) shows that at 0.001 , 0.009 and 0.001the significant terms for the variation of UTS
- ANOVA results for YTS(R2) shows that at 0.0011 , 0.001 and 0.0012 the significant terms for the variation of UTS
- ANOVA results for EL(R3) shows that at 0.0296 , 0.0488 and 0.0345the significant terms for the variation of UTS
- Maximum UTS(R1) is 403.8 at the combination of 1500 rpm rotating speed, 35 mm/min welding speed and 2 degree of tilt angle
- Maximum YTS(R2) is 348.1 at the combination of 1500 rpm rotating speed, 35 mm/min welding speed and 2 degree of tilt angle
- Maximum EL(R3) is 18.9 at the combination of 1500 rpm rotating speed, 35 mm/min welding speed and 2 degree of tilt angle

REFERENCES

[1] Abnar, B., Kazeminezhad, M., & Kokabi, A. H. (2015). Effects of heat input in friction stir welding on microstructure and mechanical properties of AA3003-H18 plates. Transactions of Nonferrous Metals Society of China, 25(7), pp 2147–2155.

[2] Huang, H. W., & Ou, B. L. (2009). Evolution of precipitation during different homogenization treatments in a 3003 aluminum alloy. Materials and Design, 30(7), pp 2685–2692.

[3] Jaradeh, M. M. R., & Carlberg, T. (2011). Solidification Studies of 3003 Aluminium Alloys with Cu and Zr Additions. Journal of Materials Science and Technology, 27(7), pp 615–627.

[4] Moreira, P. M. G. P., de Jesus, A. M. P., Ribeiro, A. S., & de Castro, P. M. S. T. (2008). Fatigue crack growth in friction stir welds of 6082-T6 and 6061-T6 aluminium alloys: A comparison. Theoretical and Applied Fracture Mechanics, 50(2), pp 81–91.

[5] Moshwan, R., Yusof, F., Hassan, M. A., & Rahmat, S. M. (2015). Effect of tool rotational speed on force generation, microstructure and mechanical properties of friction stir welded Al-Mg-Cr-Mn (AA 5052-O) alloy. Materials and Design, 66, pp 118–128.

[6] Mohammadzadeh Jamalian, H., Farahani, M., Besharati Givi, M. K., & Aghaei Vafaei, M. (2015). Study on the effects of friction stir welding process parameters on the microstructure and mechanical properties of 5086-H34 aluminum welded joints. The International Journal of Advanced Manufacturing Technology, 83, pp 611–621.

[7] Babajanzade Roshan, S., Behboodi Jooibari, M., Teimouri, R., Asgharzadeh-Ahmadi, G., Falahati-Naghibi, M., & Sohrabpoor, H. (2013). Optimization of friction stir welding process of AA7075 aluminum alloy to achieve desirable mechanical properties using ANFIS models and simulated annealing algorithm. International Journal of Advanced Manufacturing Technology, 69(5–8), pp 1803–1818.

[8] Lee, W.-B., Yeon, Y.-M., & Jung, S.-B. (2004). Mechanical Properties Related to Microstructural Variation of 6061 Al Alloy Joints by Friction Stir Welding. Materials Transactions, 45(5), pp1700–1705.

[9] Ilangovan, M., Rajendra Boopathy, S., & Balasubramanian, V. (2015). Effect of tool pin profile on microstructure and tensile properties of friction stir welded dissimilar AA 6061–AA 5086 aluminium alloy joints. Defence Technology, 11(2), pp 174–184.

[10] Krasnowski, K., Hamilton, C., & Dymek, S. (2015). In fl uence of the tool shape and weld con fi guration on microstructure and mechanical properties of the Al 6082 alloy FSW joints. Archives of Civil and Mechanical Engineering, 15, pp 133-141.

[11] Murali Krishna, P., Ramanaiah, N., & Prasada Rao, K. (2013). Optimization of process parameters for friction Stir welding of dissimilar Aluminum alloys (AA2024 - T6 and AA6351-T6) by using Taguchi method. International Journal of Industrial Engineering Computations, 4(1), pp 71–80.

[12] Kalemba, I., & Dymek, S. (2015). Microstructure and properties of friction stir welded aluminium alloys. Welding International,30(1), pp 38-42.

[13] Garg, R.K., Sharma, K., Nagpal, C.K., Garg, R., Garg, R. and Kumar, R., (2013). Ranking of software engineering metrics by fuzzy-based matrix methodology. Software Testing, Verification and Reliability, 23(2), pp.149-168.

[14] Garg, R.K., Gupta, V.K. and Agrawal, V.P., (2007). Quality evaluation of a thermal power plant by graph-theoretical methodology. International journal of power & energy systems, 27(1), pp.42.
[15] Garg, R.K., Sharma, K., Nagpal, C.K., Garg, R., Garg, R. and Kumar, R., (2013). Ranking of software engineering metrics by fuzzy-based matrix methodology. Software Testing, Verification and Reliability, 23(2), pp.149-168.

